Sulfonated Polyimide Ionomers: A Structural Study

Wafa Essafi,*,† Gérard Gebel,† and Régis Mercier‡

DRFMC-SI3M-Groupe Polymères Conducteurs Ioniques, CEA/Grenoble, UMR 5819, CEA-CNRS-UJF, 17 rue des Martyrs, 38054 Grenoble Cedex 9, France, and Laboratoire des Matériaux Organiques aux Propriétés Spécifiques, UMR 5041, CNRS, BP 24, 69390 Vernaison, France

Received July 9, 2003; Revised Manuscript Received November 5, 2003

ABSTRACT: The morphology of a series of sulfonated polyimide ionomers was investigated by small-angle X-ray and neutron scattering (SAXS and SANS) as a function of different parameters such as the ionic content, the ionic groups distribution, and the flexibility of the polymer chain. Both SAXS and SANS data exhibit the presence of an ionomer peak, indicating the presence of large ionic domains for most of the polymers. The dimension and the distribution of the ionic aggregates depend significantly on the ionic groups distribution along the polymer, and no structural evolution at nanoscopic scale accompanies the swelling process. It was found that the Dreyfus local order model where the structure of the ionic domains is locally ordered with a first four neighbors followed by a gaslike structure distribution, reproduces well our experimental data. On the other hand, the ionomer peak is not observed for very rigid polymers despite the presence of large ionic domains.

I. Introduction

Ionomers are ion-containing polymers presenting a low ion-exchange capacity.[1,2] It is generally agreed that the ion pairs form multiplets that aggregate in larger entities called clusters[3,4] which are embedded in the hydrophobic polymer matrix, resulting in a nanophase separation.[5] While the spectroscopic techniques have been widely used to study the internal structure of the multiplets and clusters,[6−9] small-angle X-ray and neutron scattering (SAXS and SANS) techniques have been shown to be well-suited techniques for the structural investigation of the size and the distribution of the clusters within the material. The SAXS or SANS spectra of ionomers usually exhibit a small-angle scattering maximum in intensity called the ionomer peak. Several models[10,11,4] were proposed considering that the ionomer peak originates from either the shape of the clusters or their spatial distribution. In the presence of water, the clusters swell, inducing a shift of the ionomer peak position toward lower angles. However, the structural evolution cannot be easily exploited to discriminate between the proposed models since both the size and the interdomain distance are modified. Due to the industrial interest of ionomers, the SAXS and SANS studies were first conducted on commercial polymers such as polyethylene (or polybutadiene) based ionomers and perfluorinated ionomers. However, the difficulty in the interpretation of the SAXS data combined with the necessity to be able to vary structural parameters has led to the investigation of some model systems such as polystyrene or polyurethane ionomers. Most of the ionomers are either random copolymers or prepared by partial postsulfonation of a neutral polymer. Therefore, the distribution of the ionic groups along the polymer chain is not controlled. Another approach was the study of model copolymers in which the ionic groups are located at the end of the polymer chain such as the halatotelechelic ionomers[12] or more recently the ABA block copolymers.[13] These studies confirmed that the origin of the ionomer peak should be attributed to the spatial distribution of the clusters. However, it is somewhat questionable how such model compounds which are water soluble and lead to ordered structures can mimic the structural behavior of actual ionomers.

The aim of studying the structure of ionomers is to determine the relationships between the microstructure and the macroscopic properties such as the mechanical properties or the ionic conductivity. It is very important to be able to modulate the structure by varying well-defined structural parameters. A new class of ionomers, the sulfonated polyimides (SPIs), has been synthesized to be used as proton conducting membranes in electrochemical systems such as H_2/O_2 fuel cells.[14−19] The polymerization method is a two-step polycondensation; namely, small ionic groups containing oligomers were first synthesized, and then, in a second step, these ionic sequences were spaced by neutral and hydrophobic sequences of controlled length on average. The polymer is then composed of alternating hydrophilic and hydrophobic sequences. It is thus possible to vary independently the length of the ionic or the hydrophobic sequences and also to use different monomers in each sequence, to modify the properties of each sequence. These polymers are not water soluble even at high temperatures probably due to the entanglements of the polymer chains in the hydrophobic sequences. In addition to this property, the control of the ionic distribution along the polymer chain makes them better model compounds for industrial ionomers than the halatotelechelic ionomers or the triblock polymers.

In the literature, two families of SPIs are described: the phthalic SPIs are characterized by five-membered imide rings, while the naphthalenic SPIs contain six-membered imide rings. Most of the studies focus on the naphthalenic SPIs because they present a higher stability and a better conductivity. A preliminary structural study by SANS has pointed out the presence of an intense ionomer peak at very low angles for the phthalic SPIs, while the naphthalenic SPIs exhibit a strong scattering at long angles, but no peak was observed. A recent study[20] using micro-SAXS experiments has shown that the structure of naphthalenic SPIs is highly aniso-

* To whom correspondence should be addressed at LPMC, Parc Valrose, 06108 Nice, France. E-mail: w.essafi@wanadoo.fr.
† CEA/Grenoble.
‡ Laboratoire des Matériaux Organiques aux Propriétés Spécifiques.

10.1021/ma034965p CCC: $27.50
Published on Web 12/31/2003

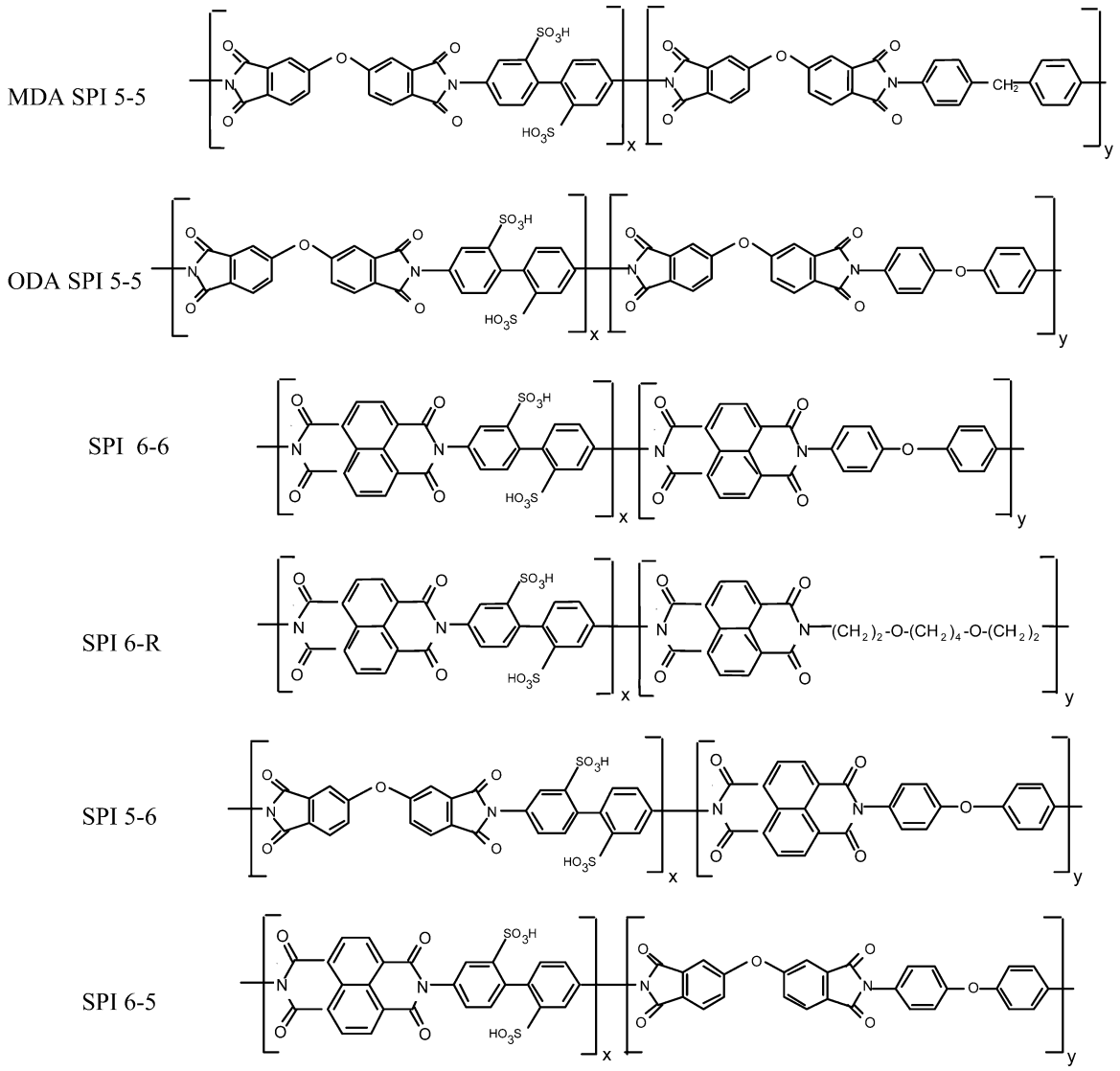

Figure 1. Chemical structure of the polymers used in this study.

tropic, and the results were interpreted as originating from a multiscale foliated structure which induces anisotropic transport properties. Contrary to naphthalenic SPIs, the swelling properties of phthalic SPIs are isotropic along the three directions. These results can be attributed to differences in the polymer chain flexibility. The aim of the present work is to study the structural evolution of the sulfonated polyimide membranes using both SAXS and SANS as a function of different parameters such as the nature of the counterion, the charge content, the charge distribution along the polymer chain and the flexibility of the chain.

II. Experimental Section

II.1. Copolymer Synthesis. All the monomers and solvents were obtained from commercial sources. They were purified to obtain polymers presenting a molecular weight as large as possible. The sulfonated monomer BDSA (4,4′-diamino-2,2′-biphenyldisulfonic acid) was treated with charcoal in water and dried under vacuum at 100 °C. The phthalic dianhydride ODPA (oxydiphthalic dianhydride) and the neutral diamine ODA (4,4-oxydianiline) were purified prior to use by vacuum sublimation. The naphthalenic dianhydride NTDA (naphthalene-1,4,5,8-tetracarboxylic acid dianhydride) was dried at 160 °C under vacuum. The BDSA was neutralized with triethylamine to obtain a soluble monomer.

Several families of sulfonated polyimides whose chemical formulas are presented in Figure 1 have been prepared according to a procedure reported elsewhere.[14,18,21,22] The method consists of a two-step polycondensation of aromatic diamines and dianhydrides. In a first step, the sulfonated diamine BDSA is polymerized either with dianhydride ODPA in *m*-cresol at 200 °C or with NTDA in cosolvent system phenol/chlorophenol at 160 °C. An excess of BDSA was introduced to control the average length of the ionic sequence. In a second step, the remaining dianhydride monomers ODPA or NTDA were introduced with the diamine ODA to space the ionic blocks by hydrophobic sequences and to control the ion exchange capacity.

The phthalic polyimides based on BDSA, ODPA, and ODA as monomers are called ODA SPI 5-5 (Figure 1). A series of polymers presenting five repeat units on average in the ionic sequence ($x = 5$ in the chemical formula) and varying the y value to get x/y ratios ranging from 20/80 to 60/40, was prepared. A second series was synthesized varying the x value from 1 to 5 with a constant x/y ratio ($x/y = 30/70$). Another polymer called MDA SPI 5-5 (Figure 1) was synthesized by replacing the neutral diamine ODA by MDA (4,4′-diamino-2,2′-diphenylmethane), so the methyl group of MDA has replaced the oxygen in the ether bridge of ODA.

A more rigid sulfonated polyimide called SPI 6-6 (Figure 1) was prepared with $x = 5$ and $x/y = 30/70$ using a naphthalenic dianhydride, NDTA, as monomer in both sequences. To study the effect of the polymer chain flexibility and to favor the phase separation between the two sequences, the aromatic diamine used in the hydrophobic sequence was replaced by an aliphatic one, BOE (2,2′-[1,4-butanediylbis(oxy)]bisethanamine), to yield

Table 1. [a]

monomer	ODA	ODA	ODA	ODA	ODA	ODA	ODA	ODA	MDA
x	1	3	4	5	5	5	5	5	5
x/y	30/70	30/70	30/70	20/80	30/70	40/60	50/50	60/40	30/70
EW (g/equiv)	862	862	862	1256	862	667	546	465	860
$\Delta M/M$ (%)	15	17	21	12.3	15.3	26.3	29	37	28
$n(H_2O/SO_3^-)$	7.1	8.1	9.9	8.6	7.3	9.8	8.7	9.7	13.4
σ (10^{-3} S cm^{-1})	0.21	2.9	5.5	0.84	1.4	6.0	18	27	
ϕ_w		0.22	0.27		0.20	0.33	0.36	0.45	0.35
R (Å)		84	115		127	132	115	124	107
D (Å)		193	248		302	269	225	226	228
z		4.66	4.7		4.65	4.76	4.79	4.75	4.8
α		1.168	1.18		1.18	1.165	1.144	1.145	1.14

[a] x is the average number of charged units in the ionic sequences, x/y is the molar ratio of charged to neutral units, EW is the equivalent weight, ΔM/M is the water uptake percentage, n is the number of water molecules per ionic group, σ is the ionic conductivity, ϕ_w is the water volume fraction, R is the radius of the ionic domains, D is the distance between the ionic domains, z is the number of missed ionic domains due to the existence of the correlation hole of size α in the radial distribution function of the local order model.

SPI 6-R (Figure 1). Also, mixed phthalic/naphthalenic sulfonated polyimides SPI 6-5 and SPI 5-6 (Figure 1) based on NDTA, ODPA, BDSA, and ODA as monomers have been prepared in the same conditions as SPI 6-6; their x value = 5 and x/y = 30/70.

II.2. Film Preparation. The SPI films were obtained by casting on a glass plate from a 5% w/w polymer solution in *m*-cresol for the phthalic SPIs and in chlorophenol for the naphthalenic SPI. The solvent was then evaporated under vacuum at 150−170 °C for 1 day. The polymer films were then rinsed several times with hot methanol and water. The polymer films obtained on a triethylammonium form were exchanged by soaking the films in a chloride solution of the desired monovalent cation for 2 h. The polymer films were then rinsed several times with pure water and dried under vacuum at 150 °C for 3 h.

II.3. Membrane Characterization. The amount of water absorbed in phthalic SPI membranes was determined gravimetrically for various membranes presenting different equivalent weights EW (EW is the mass of the dry polymer per ionic group, i.e., SO_3^-) from 465 to 1256 g/equiv with the same ionic sequence length (x = 5) and for membranes presenting different ionic sequence lengths from x = 1 to x = 5 with the same equivalent weight, EW = 862 g/equiv. Membranes were weighed in both the dry and swollen states. Wetted membranes were blotted dry with filter paper to remove excess water. Measurements were repeated until reproducible values were obtained. The weight increase was calculated with respect to the dry membrane weight ($\Delta M/M$). Polymers presenting a large ionic content (x/y > 40/60) exhibit very poor mechanical properties in the swollen state due to the large water content. They are thus difficult to handle, increasing the experimental errors on swelling data. The water uptakes can also be expressed as the number of water molecules per ionic group, $n = (\Delta M/M)(EW/18)$. The striking result of these swelling measurements reported in Table 1 for SPI 5-5 polymers is the relative constancy of the n value ($n \approx 8-9$) over a wide range of the ionic content (from EW = 465 g/equiv to EW = 1256 g/equiv). According to our knowledge this behavior had never before been observed on such a wide range of EW. For typical membranes, the n value significantly increases in the case of the usual membranes such as PFSI and even diverges for large ion content since the membrane dissolves in water at room temperature.[23−26] The fact that n values for PIS membranes are independent of ion content suggests that most of the solvent (water) is located in the ionic domains since the filling of a macrosopic porosity or a significant hydration of the hydrophobic part of the polymer will not lead to a constant n value. Moreover, the morphology along thickness was studied on cryofractured membranes using a JEOL SM840 scanning electron microscope, and the absence of macroscopic porosity was verified.

For X-ray and neutron scattering analysis, the water content has to be expressed as the water volume fraction, which requires the knowledge of the polymer density. It was experimentally determined by the comparison of the weight and volume of a water-swollen membrane assuming a two-phase separation, with use of a picnometer. This value (1.4 g/cm^3) was confirmed by the determination of the *m*-cresol solution density at various polymer concentrations from 1% to 5% using a PAAR DMA 35 densitimeter.

The conductivity measurements were performed using a cell with mercury electrodes (electrode diameter 0.283 cm^2) by impedance measurement using a Solartron Instrument SI1255 as frequency analyzer and a Paar 273 as potentiostat. The explored frequency range was typically 1−500 kHz. The electrical resistance of the swollen membranes was determined when the imaginary part of the impedance was equal to zero. The impedance diagrams are typical of highly conducting membranes.[27]

The broad-line ^{1}H NMR spectra of the membranes in the dry and swollen states were recorded on a Brucker CXP 90. The membranes previously dried for 1 day at 80 °C under vacuum were swollen in D_2O, and the solvent was renewed several times to avoid the presence of protons in the water.

II.4. Small-Angle Scattering Data. The small-angle neutron scattering experiments were performed on the PAXE spectrometer at the Laboratoire Léon Brillouin (CEA-CNRS, Orphée reactor, Saclay, France). The scattering vector is defined as $q = 4\pi \sin(\theta/\lambda)$, where θ is the scattering angle and λ is the neutron incident wavelength. The explored q range was varied from 0.008 to 0.3 Å^{-1} using two different configurations: (i) λ = 12 Å and D = 5 m as the sample to detector distance, (ii) λ = 5 Å and D = 2 m for the large q values. The cells were formed by two quartz windows spaced by a quartz ring of 1 mm thickness. Usual corrections for background subtraction and detector normalization were applied to the data.

The small-angle X-ray scattering experiments were performed on the D22 spectrometer at the Laboratoire LURE (CEA-CNRS-MRT, Orsay, France). The spectrometer is equipped with a one-dimensional position-sensitive detector. The double-crystal monochromator was turned to provide a beam of 8500 eV X-rays (λ = 1.46 Å). The sample-to-detector distance at 2 m allowed SAXS data to be in the q range from 0.008 to 0.25 Å^{-1}. The membranes were studied in cells with Kapton windows.

The ultra-small-angle X-ray scattering (USAXS) spectra were recorded on a double-crystal multiple-reflection camera. The X-ray beam, produced by a RU 300 rotating anode from Rigaku at 18 kW with a Cu Kα target, coming out of the monochromator, crosses the sample and is then analyzed by a scintillator rotating around the analyzer axis. The monochromator and the analyzer are identical multiple-reflection channel-cut crystals. The apparatus and the data desmearing method are described in detail elsewhere.[28,29]

Membrane samples were investigated in the dry state after treatment under vacuum at 100 °C for 12 h or at room humidity or in the D_2O or H_2O swollen state.

III. Results and Discussion

III.1. Comparison between SAXS and SANS. The scattering profiles normalized by the scattering invari-

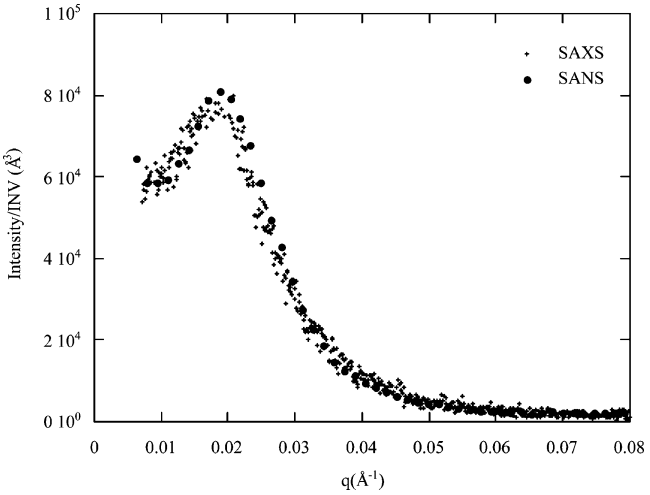

Figure 2. SAXS and SANS profiles normalized by the scattering invariant of ODA SPI 5-5 ($x = 5$, $x/y = 30/70$) at room humidity.

ant of ODA SPI 5-5 ($x = 5$, $x/y = 30/70$) at room humidity, obtained by both SAXS and SANS, are shown in Figure 2. The scattering invariant, INV, is defined as

$$\mathrm{INV} = \int_0^\infty q^2\, I(q)\, \mathrm{d}q = (\Delta\rho)^2\phi(1-\phi)2\pi^2 \qquad (1)$$

The second part of the equation is true only for a two-phase system where ϕ is the volume fraction of one phase. The invariant is used to normalize the scattered intensities and to eliminate the contrast term specific for each radiation and which is difficult to determine experimentally or to calulate.

The ODA SPI 5-5 SAXS and SANS profiles at room humidity are exactly superimposable once normalized by the scattering invariant. It emerges that the image of the ionic domains focusing on the counterions (SAXS) is the same as that given by the water trapped in SANS, and thus, the distributions of both the water molecules and the ionic groups are identical within the ionic aggregates. This observation indicates that the system can be analyzed as a two-phase system: ionic domains and polymeric matrix.

The ionomer membranes are characterized by a nanophase separation leading to ionic domains embedded in the hydrophobic domains. The water picked up from the atmosphere is trapped in the ionic domains (hydrophilic). In SANS, the contrast arises from the difference of the scattering length density between the polymeric matrix ($b/V \approx 2.7 \times 10^{10}$ cm^{-2}) and the water ($b/V \approx -0.56 \times 10^{10}$ cm^{-2}). However, in SAXS the contrast mainly arises from the difference of the electronic density between the polymeric matrix ($Z/V \approx 0.39$ e/Å^3) and the ionic groups (in the case of $-SO_3Na$, $Z/V \approx 0.75$ e/Å^3).

The scattering profiles exhibit the presence of a peak at low angles; $q_{max} = 0.02$ Å^{-1}. As previously observed, this peak position is very low compared to those of other ionomers such as Nafion,[30] for which the peak position is found to be around $q_{max} = 0.1-0.2$ Å^{-1} depending on the water content. Since these membranes exhibit a significant ionic conductivity in the swollen state, the ionic domains should percolate and it can be deduced that their size is roughly 10 times larger than that of usual ionomers. This result can obviously be attributed to the block character of the polymers.

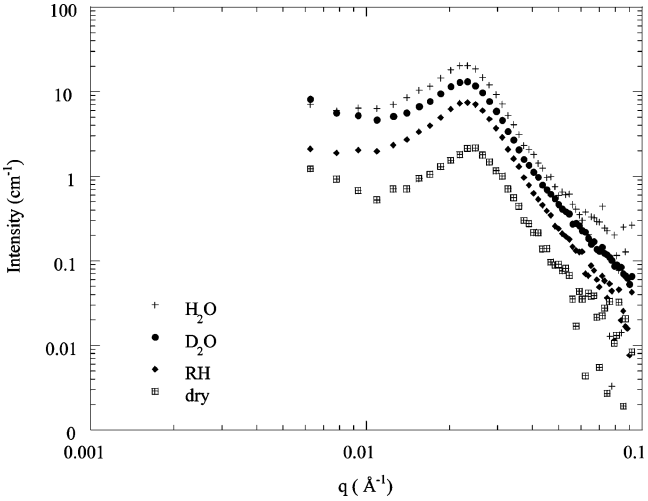

Figure 3. SANS spectra of MDA SPI 5-5 ($x = 5$, $x/y = 30/70$) as a function of water content (proton form).

The spectra plotted on a double-logarithmic scale exhibit an asymptotic behavior at large angles scaling as q^{-4}, which is characteristic of scatterers presenting a well-defined interface with the polymer matrix (Figure 3). From this asymptotic behavior of the scattering curves, the quantity of the interface can be extracted through the relation[31]

$$\lim_{q\to\infty} Iq^4 = 2\pi(\Delta\rho)^2\Sigma = \frac{\Sigma(\mathrm{INV})}{\pi\phi_i(1-\phi_i)} \qquad (2)$$

where ϕ_i is the volume fraction of the scattering ionic domains, $(\Delta\rho)^2$ is the contrast, and Σ is the surface of the interface over the total volume. It is important to note that the Σ determination is not model dependent. The size of the scattering particles can be extracted from the Σ value assuming a spherical geometry for the scattering domains; their radius is given by the following formula:

$$R = \frac{3\phi_i}{\Sigma} \qquad (3)$$

Combining eqs 2 and 3 and introducing the experimental value of the Porod limit normalized by the invariant, $\lim_{q\to\infty} Iq^4/\mathrm{INV}$, and that of ϕ_i ($\phi_i \approx 40\%$), an approximate value of 120 Å for the radius of the ionic domains can be extracted. This value for the SPI is 6 times larger than the one determined for Nafion,[11,32] confirming the existence of larger ionic domains as determined from the ionomer peak position.

Another indication of the presence of large ionic domains can be deduced from the level of the scattered intensities. The maximum of intensity of the ionomer peak is about 8.6×10^4 Å^3 for SPI, while the value determined for Nafion is about 8×10^2 Å^3 (108 times higher). The scattered intensity is proportional to the scattering domains volume and hence to their cubic radius (R^3), and we deduce from this intensity ratio that the radius of the scattered SPI domains is about $108^{1/3} \approx 5$ times bigger than that of the Nafion domains. This is a crude determination since it does not take into account the effect of the variation of the number of scattering particles on the scattered intensity. However, this contribution is mostly compensated by the normalization by the scattering invariant. Moreover, the extracted value is in good agreement with the previous

ones obtained by the analysis at large-angle asymptotic behavior as well as with the peak position q_{max}, confirming that the entire scattering profile reveals the existence of very large ionic domains. The studied SPI polymer is constituted by a series of blocks of five units ($x = 5$), giving rise to ionic domains about 5 times bigger than that of Nafion. It is then possible to modulate the dimension of the ionic domains by varying the distribution of the ionic groups along the polymer chain.

III.2. Effect of Water Content. Figure 3 shows the evolution of the SANS profiles obtained for MDA SPI 5-5 membranes ($x = 5$, $x/y = 30/70$) in the dry, room humidity equilibrated, and water (H_2O and D_2O) swollen states. The most striking result is the absence of shape modification of the profiles accompanying the swelling process. The only modification of the scattering profiles due to water uptake is an increase of the scattered intensity level due to the modification of the contrast between the polymer matrix and the ionic domains. The main consequence of this result is that the swelling does not affect the local structure on a nanometer scale and corresponds only to the filling of the ionic domains. Thus, the variation of the water uptake is not a relevant parameter to study the structure of SPIs, and it is not necessary to carefully control and determine its value.

The levels of scattered intensity obtained for membranes equilibrated with either H_2O or D_2O are very close. The same result was obtained for experiments performed with polymers presenting different ion contents and distributions. It follows that the contrast between the ionic phase and the polymer matrix (and consequently the composition of both phases) does not depend on the charge content or the charge distribution. This result is not surprising since the scattering length density of the polymeric matrix is expected to be between those of H_2O and D_2O. So, if the charge content or the charge distribution is varied, the compositions of the ionic phase and the hydrophobic matrix remain constant; however, the geometry of the system is modified.

In the absence of structural evolution upon swelling, the ionic domains in the hydrated state cannot be water pools but should contain a homogeneous distribution of the polymer chains wearing the ionic groups as shown by the evolution of the scattered intensity with the water content and the fact that the SAXS and SANS spectra are identical.

It is worth noting that the same experiments performed with SANS with Nafion membranes reveal strong differences between the spectra obtained in H_2O and D_2O due to the counterion condensation at the polymer/water interface.[33]

III.3. Effect of the Counterions. The ODA SPI 5-5 characterized by $x = 5$ and $x/y = 30/70$ was neutralized with various counterions, such as TEA (tetraethylammonium), Li^+, Na^+, K^+, and Cs^+.

Figure 4 shows the evolution of the SAXS spectra of ODA SPI 5-5 at room humidity as a function of different monovalent counterions. The ionomer peak position is independent of the monovalent counterion; however, its intensity is increased as the atomic number Z of the counterion increases due to an increase of the contrast. For the alkaline counterions, the ratio of the intensity of the scattering maximum for two different counterions is directly proportional to the square of the atomic number ratio of these counterions. This behavior indicates also that the contrast arises mainly from the counterions within the ionic domains; once again we confirm that the peak is an ionomer one. The upturn observed at very small angles is classical and was usually observed for ionomers. It is now attributed to large-scale density fluctuations of scatterers.[32,34,35]

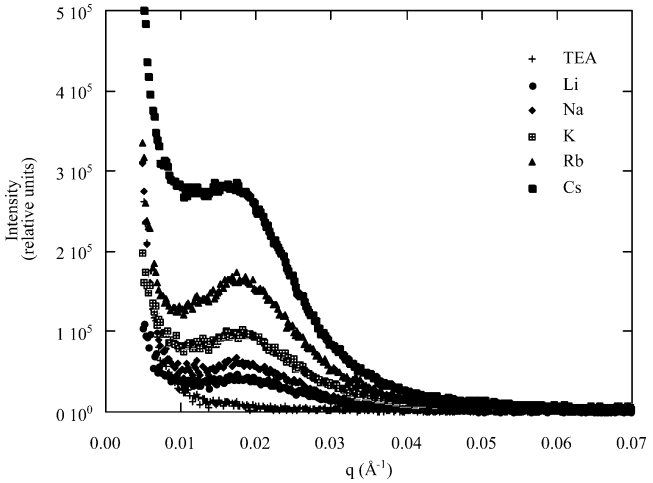

Figure 4. SAXS profiles of ODA SPI 5-5 ($x = 5$, $x/y = 30/70$) at room humidity as a function of various monovalent counterions.

The ionomer peak cannot be observed for the triethylammonium form by SAXS because of the low contrast value. On the contrary, the SANS profile obtained for the same sample clearly reveals a well-defined ionomer peak as observed for the proton form in Figure 3 due to the presence of a large number of protons which increase the scattering length density difference with the polyaromatic matrix.

III.4. Effect of the Charge Content. The charge content was varied by varying the length of the hydrophobic sequence while keeping constant the ionic sequence length. A series of ODA SPI 5-5 ($x = 5$) polymers has been synthesized using the same protocol for the first step of the synthesis, and the length of the hydrophobic sequence (related to the y value) was then varied in the second step of the synthesis (as y decreases, the charge content increases). The polymers are characterized by the x/y ratio, which was varied from 20/80 to 60/40. The membranes were neutralized with CsCl to get a good contrast for SAXS and kept dried under vacuum for the SAXS investigation.

The SAXS data shown in Figure 5 reveal the presence of a peak in the scattering profiles for all the charge content from $x/y = 20/80$ to $x/y = 60/40$. The peak is shifted slightly to lower q as the charge content decreases (x/y decreases), while its intensity $I(q_{max})$ and the intensity scattered at zero angles $I(q \rightarrow 0)$ increase.

The effect of increasing the spacing between the ionic sequences (the charge content decreases) causes a shift of the ionomer peak toward smaller q values; this behavior reflects that the distance between ionic domains increases. Such a result favors the interparticular origin for the ionomer peak. Indeed, in the case of an intraparticular origin of the peak, it is expected that all the spectra present the same shape and the only modification should be the level of the scattered intensity because the same scattering objects should be observed with a number proportional to the charge content.

Assuming that the size of the ionic domains is only defined by the nature of the ionic sequence (length,

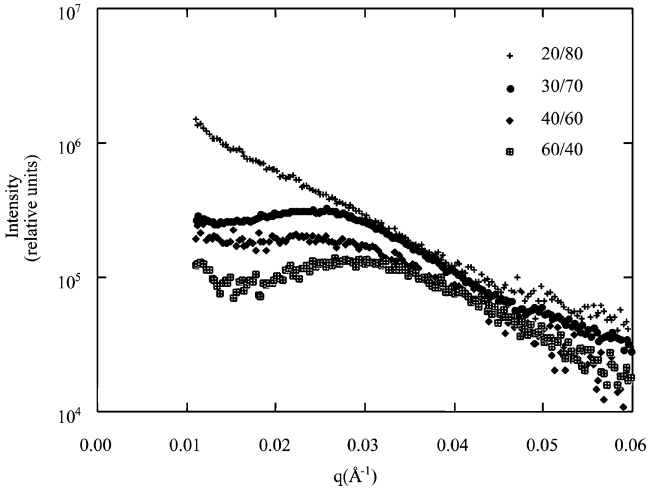

Figure 5. SAXS profiles of dried ODA SPI 5-5 ($x = 5$) (cesium form) as a function of the charge content (x/y varies from 20/80 to 60/40).

rigidity, ...) and neglecting the increase in conformational constraints consecutive to the decrease of the nonionic chain length, if we assume a diamond-like structure "tetrahedral coordination" to agree with the percolation threshold at low water content,[36] the first neighbors distance D is given by the following formula:

$$D = \left(\frac{(\sqrt{3})\pi}{2\phi_i}\right)^{1/3} R \qquad (4)$$

R is the radius of the ionic domains, and ϕ_i is their volume fraction.

The shift of the ionomer peak position is expected to vary as the power 1/3 of the increase of the ionic domains volume fraction, in agreement with the experimental results despite the difficulty to pick up precisely the peak position with such broad scattering maxima and its modification by the presence of the small-angle scattering upturn.

III.5. Effect of the Charge Distribution. The charge distribution was varied by varying the ionic sequence length; the x value varies from 1 (one ionic monomer per ionic sequence on average; it deals with the statistical polymer) to 5 sulfonated monomers per ionic sequence, while the charge content was kept constant (the ratio x/y is fixed to 30/70).

Figure 6 shows the evolution of the corresponding SAXS profiles of the ODA SPI 5-5 (cesium form) at room humidity as a function of the charge distribution. As expected, the evolution of the scattering profiles is very pronounced with the charge distribution compared to the effect of the charge content. As the ionic sequence length (related to the x value) decreases, the peak shifts to higher q; at the same time its intensity $I(q_{max})$ and the intensity scattered at zero angle $I(q \rightarrow 0)$ decrease. This behavior is in agreement with smaller and closer scattering ionic domains as the ionic sequence length decreases. According to eq 4, the dependence of the peak position q_{max} on the size of the ionic domains R is strong: $q_{max} \propto 1/R$. Indeed, since the charge content is constant, the volume fraction of the scattering ionic domains ϕ_i is constant with the charge distribution, so the first neighbors distance D depends only on the radius R (proportional to R), and as a consequence, the peak position is proportional to $1/R$ (the plot of q_{max} as a function of R should be a straight line).

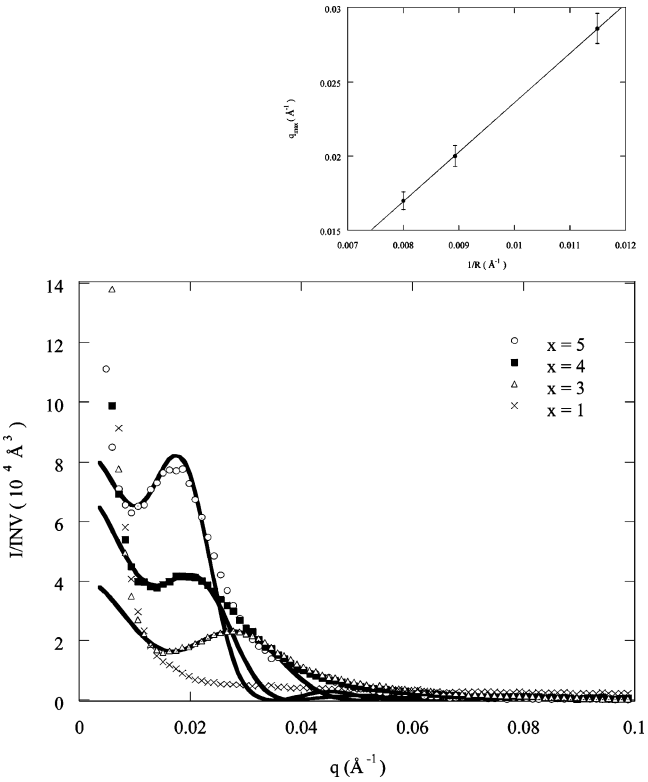

Figure 6. SAXS profiles of ODA SPI 5-5 ($x/y = 30/70$) (cesium form) at room humidity as a function of the charge distribution ($x = 5$, $x = 4$, $x = 3$, and $x = 1$) and their adjustment according to the local order model. The inset corresponds to the evolution of q_{max} as a function of the inverse of the ionic domains radius ($1/R$) ($x = 5$, $x = 4$, and $x = 3$).

The radii of the ionic domains were calculated according to eq 3 for the different x values, and the evolution of q_{max} as a function of $1/R$ and the corresponding linear fit are shown in the inset of Figure 6 (note that we have only three experimental points).

On the other hand, no ionomer peak is observed for the statistical polymer; this result can be interpreted by the fact that either the ionic groups are dispersed in the polymer matrix or the ionic domains are not large enough to give rise to a visible peak. It should be noted that the synthesis method of the statistical polymer is different from that of the block copolymers since it is prepared using only one-step polycondensation, which could lead to a different structure.

III.6. Analysis of the Scattering Curves Using the Local Order Model. The local order model was previously developed for perfluorinated ionomer membranes[32,37] and used to analyze the SANS and SAXS profiles to extract structural parameters (cavity radius and interdomain distance). The primary ideas of this model are to consider that the aggregates are spherical and well-ordered on a local scale and that the order rapidly vanishes for longer distances. The ionic aggregation is thermodynamically favored, and in the absence of topological constraints, the spherical shape allows the minimization of the interfacial energy between the internal ionic solution and the hydrophobic polymer matrix. The local ordering is considered as a consequence of the average distribution of the ionic blocks along the polymer chain; namely, the existence of an ionic domain increases significantly the probability of finding other domains at a well-defined distance in its vicinity. The absence of long-range order was de-

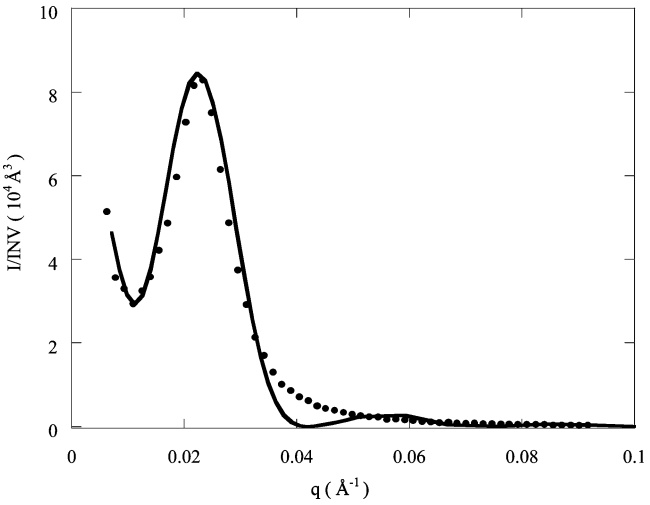

Figure 7. SANS profile of the proton form of MDA SPI 5-5 ($x = 5$ and $x/y = 30/70$) in D_2O and its adjustment according to the local order model.

duced from the width of the scattering maximum and the absence of highest order diffraction peaks. A simplified radial distribution function (RDF) was constructed which is composed of a correlation hole at short distances containing a Dirac peak (the first neighbors) followed by a constant probability of finding the following neighbors. The coordination number (number of first neighbors) was previously chosen to be 4 to explain the existence of a percolation threshold at low water content observed for Nafion membranes through the transport properties.[38] This coordination number was confirmed by the fitting procedure of the SANS spectra,[30] and the same value was chosen in the present analysis to reduce the number of free parameters. The scattered intensity can then be written as

$$\frac{I(q)}{\mathrm{INV}} = \frac{2R^3}{3(1-\phi_w)\pi}\Phi(qR)^2\left(1 + 4\frac{\sin(qD)}{qD} - z\Phi(\alpha qD)\right) \quad (5)$$

where

$$\Phi(x) = 3\frac{\sin(x) - x\cos(x)}{x^3} \quad (6)$$

The model parameters are the aggregate radius (R), the interaggregate distance (D), the size of the correlation hole created in the RDF with respect to the distance D, (α), and the number of aggregates missing in the RDF due to the existence of the correlation hole (z). A relation between the radius and the interaggregate distance D was introduced according to eq 4 using space-filling arguments based on a diamond-like structure and the water volume fraction.[39]

As depicted in Figure 7, this model developed for perfluorinated ionomer membranes, reproduces surprisingly well the SANS curve obtained for the proton form of the MDA SPI 5-5 ($x = 5$ and $x/y = 30/70$) in D_2O with a reduced number of free parameters, since the α and z values deduced from the fitting procedure ($\alpha = 1.14$ and $z = 4.8$) are close to those determined for Nafion membranes ($\alpha = 1.155$ and $z = 4.45$). Moreover, these parameters were mainly adjusted to reproduce the small-angle upturn at very low angles. The only relevant parameter is thus the radius of the cavities, which is 5 times larger for MDA SPI 5-5 membranes ($R = 107$ Å) than that obtained for Nafion membranes ($R = 20$ Å).[32]

The model was then used to reproduce the scattering curves obtained for ODA SPIs, varying both the ion content and distribution along the polymer chain. In Figure 6, the obtained adjustments are presented for the different ionic block sequence lengths at constant charge content. A complete set of the parameters deduced from the fitting procedure for each polymer is given in Table 1 (note that we have used in the fit ϕ_w, the water volume fraction, and not ϕ_i, the ionic volume fraction, indeed we obtain roughly the same fit parameters: D is decreased by only 10% when ϕ_i is used). The main result is that the size of the ionic domain appears to be roughly proportional to the average number of ionic monomers per ionic sequence and is constant as the ionic content increases, for $x = 5$. These deductions confirm that the block character is introduced through the synthesis method and the interest of using such a simplified model to reproduce the scattering data of ionomer membranes. The second result is the comparison between the interaggregate distance and the diameter of the ionic cavities. As ionic content increases, the interdomain distance decreases, which correlates well with the increase of the ionic conductivity; namely, the ionic conductivity reaches relatively high values when the diameter value becomes close to the interdomain distance, which can be interpreted as a percolation phenomenon. The absence of an ionomer peak for the 20/80 SPI polymer does not allow use of the local order model.

The comparison between the SANS spectra obtained for MDA and ODA SPI 5-5 indicates that the ionomer peak is more marked for MDA. These two polymers do not significantly differ in their chain flexibility, but probably an effect of polymer chain solubility has to be invoked.

III.7. Effect of the Polymer Chain Flexibility. As previously reported, the naphthalenic polymer SAXS spectra do not present the ionomer peak.[22] This surprising feature does not mean that there is no ionic aggregation since the scattered intensity is very large. The first idea was to consider that the ionomer peak was located at lower q values. Ultra-small-angle scattering spectra were recorded, and no ionomer peak can be observed down to $q = 3 \times 10^{-4}$ Å^{-1} (Figure 8). Moreover, these data are analyzed as arising from large-scale density fluctuations, and the correlation length extracted from a $I^{-1/2}$ vs q^2 plot (Debye Bueche model) is $\xi \approx 1200$ Å.

The chemical formula of SPI 6-6 suggests a very rigid structure; namely, no flexibility is present in the ionic sequence, and only one flexible bond is introduced by the ether bond of the ODA monomer, in the neutral sequence. Figure 9 illustrates the rigidity of SPI 6-6 through the structure of the sequence NTDA/BDSA/NTDA/ODA and compared to that of SPI 5-5 through the sequence ODPA/BDSA/ODPA/ODA.

We should note that, in our case, the monomer is represented by the ionic sequence NTDA/BDSA in the case of SPI 6-6 and ODPA/BDSA in the case of SPI 5-5, which should be repeated 5 times ($x = 5$), and the neutral sequence NTDA/ODA in the case of SPI 6-6 and ODPA/ODA in the case of SPI 5-5, which should be repeated 11.6 times ($x/y = 30/70$). So it emerges that there is no flexibility and no possibility of rearrange-

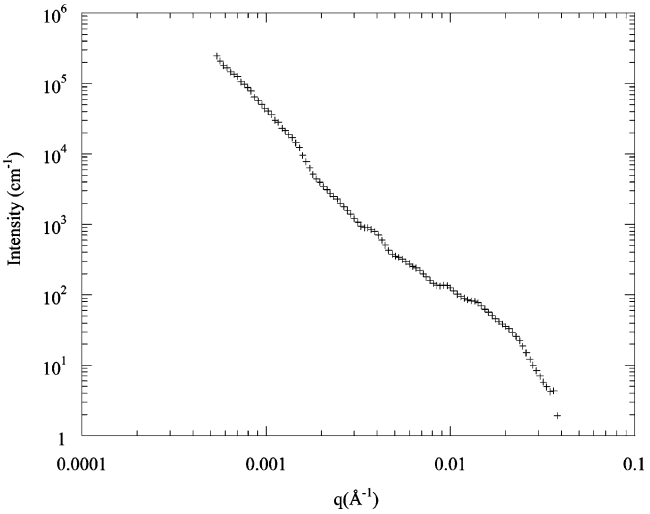

Figure 8. USAXS scattering profile of SPI 6-6 ($x = 5$, $x/y =$ 30/70) at room humidity.

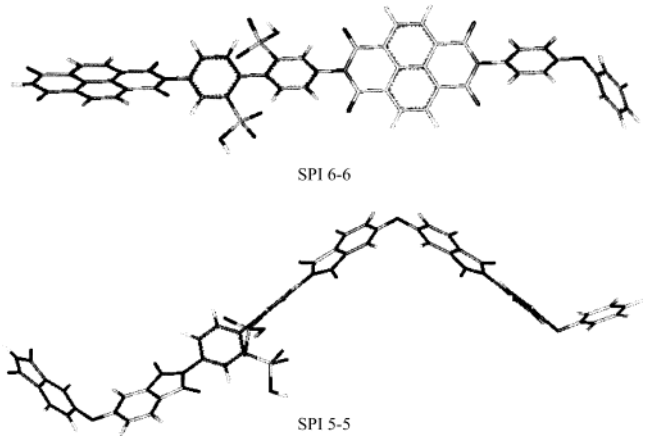

Figure 9. Structure of the sequences NTDA/BDSA/NTDA/ODA and ODPA/BDSA/ODPA/ODA.

ment in the case of SPI 6-6, as opposed to the case of the SPI 5-5. The structure was performed by the BIOSYM program, which minimizes the potentiel energy as a function of the orientation and the bond lengths.

To verify the hypothesis of the rigidity, a naphthalenic SPI 6-R (Figure 1) was synthesized using the aliphatic diamine BOE, which allows some flexibility to be introduced into the neutral sequence. The SAXS spectrum shown in Figure 10 reveals the existence of a well-defined ionomer peak at $q_{max} = 0.02$ Å^{-1}, confirming that the absence of an ionomer peak in the small-angle scattering spectra of naphthalenic ionomers is due to an excess of the polymer chain rigidity.

To further investigate the effect of the polymer chain flexibility and to determine the relative influence of the rigidity either of the ionic or of the neutral sequence, mixed phthalic and naphthalenic SPIs were synthesized (Figure 1).

Figure 11 shows the SAXS spectra of the mixed SPI (SPI 5-6, SPI 6-5) and also those of SPI 5-5 and SPI 6-6 for comparison. All these SPIs are characterized by $x =$ 5 and $x/y =$ 30/70. The peak of SPI 6-5 is more pronounced than that of SPI 5-6; the scattered intensity $I(q\rightarrow 0)$ and $I(q_{max})$ are higher for SPI 6-5. The peak position is shifted to lower q values for SPI 6-5: q_{max}(SPI 6-5) = 0.017 Å^{-1}, q_{max}(SPI 5-6) = 0.024 Å^{-1}. So, the presence of the ionomer peak is correlated to the

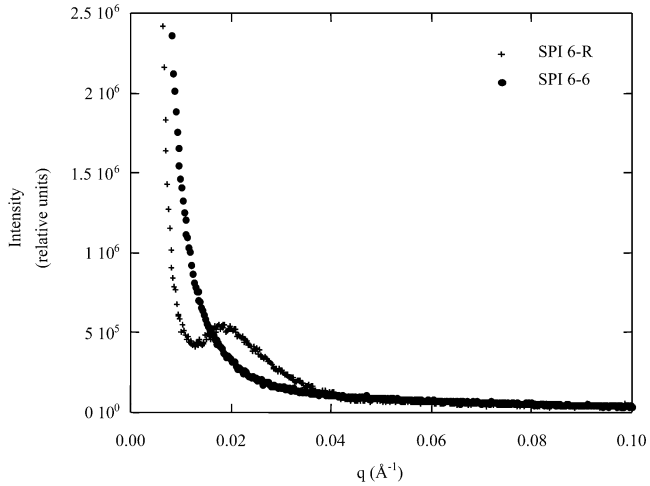

Figure 10. SAXS profile of SPI 6-R ($x = 5$, $x/y =$ 30/70) at room humidity.

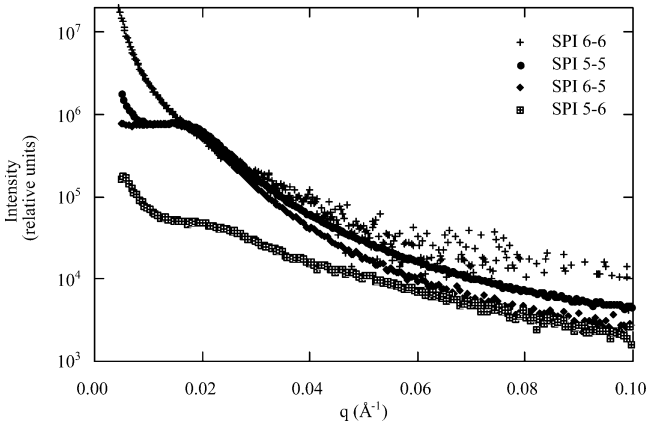

Figure 11. SAXS profiles of SPI 5-6, SPI 6-5, SPI 5-5, and SPI 6-6 ($x = 5$, $x/y =$ 30/70) at room humidity.

flexibility of the neutral sequence much more than that of the ionic sequence. This implies that the flexibility of the neutral sequence governs the reorganization of the structure and the formation of the ionic domains.

III.8. Ionic Conductivity. The ionic conductivity was determined for membranes in the acidic form and equilibrated in pure water at room temperature using a cell with mercury electrodes. The results reported in Table 1 indicate as expected that the ionic conductivity increases as the ion content increases and depends on the ion distribution along the polymer chain. Since n values are constant with varying equivalent weight, the ion concentration inside the ionic domains is constant. Therefore, the variation of the ionic conductivity is only related to an increase of the proton mobility. The local mobility will depend on the internal structure of the ionic domains, but it is expected to be very large compared to the long-range mobility due to the existence of interdomain connections as observed for the diffusion of water in PFSI membranes.[39] The ionic conductivity is a macroscopic quantity which will thus be extremely sensitive to the connection between ionic domains. Since the size and the distribution of the ionic domains will depend on both the ion content and distribution along the polymer chains, the ionic conductivity will give information on the connectivity (or tortuosity) of the system, which should strongly correlate to the microstructure. The increase of conductivity as charge content increases can be interpreted as a percolation-like behavior; namely, the ionic conductivity presents a large

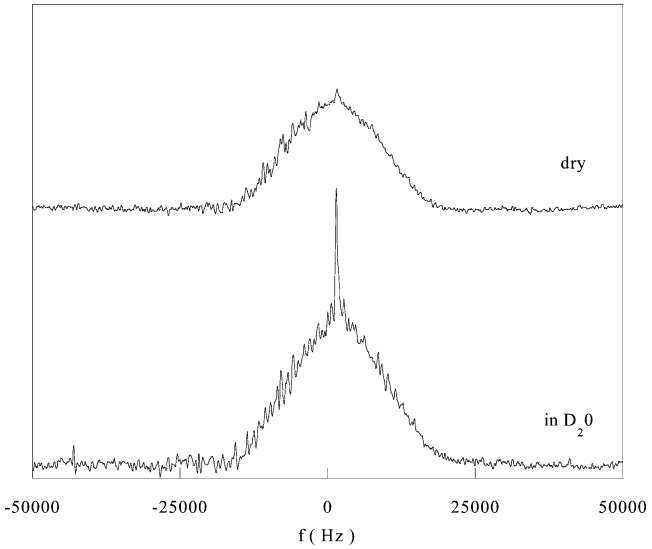

Figure 12. ^{1}H NMR spectra of dry and D_2O-swollen membranes (ODA SPI 5-5, $x = 5$, $x/y = 30/70$).

increase close to the percolation threshold of the ionic domains, and then a saturation is observed. The observation of a maximum value of the conductivity depending on the ionic sequence length at constant charge content cannot completely be attributed to the variation of the water uptake, which presents the same trend but is very small. The explanation can be found in the existence of two competitive processes. Assuming an affine evolution of the structure depending on the block character, the conductivity is expected to decrease as the block length increases owing to the increase of the interdomain connection length, which should be the limiting phenomenon in the ion transport. However, for very short sequences such as in the statistical polymer, the ionic species are probably more homogeneously distributed in the polymer matrix and do not favor the formation of a percolated ionic phase. It is worth noting that the ionic conductivities are relatively low compared to those measured for rigid polyimide structures.[16,17]

III.9. NMR Analysis. The analysis of the line shape of the ^{19}F NMR spectra of perfluorinated ionomers upon swelling revealed a modification of the NMR line shapes attributed to an increase of the polymer chain mobility upon swelling.[40−42] The NMR spectra of the dry state are characterized by a very broad line (full width at half-maximum >20 kHz) due to the absence of motion averaging. The broadening of the spectra obtained for a swollen membrane decreases as the water uptake increases. For large water content, the broad line splits into several lines whose positions are similar to those obtained with solutions. This evolution is similar to the effect of increasing temperature beyond the glass transition temperature. It was concluded that water acts as a plasticizer, which increases at least locally the polymer chain mobility.

The same type of experiments were performed on ODA SPI 5-5 membranes, and the comparison of the ^{1}H NMR spectra of dry and D_2O-swollen membranes do not reveal any difference, as shown in Figure 12. Both the shape and the line width of the broad NMR line due to the protonic part are identical, which indicates that the swelling does not induce any increase of the polymer chain motion; namely, the swelling of the ionic domains does not affect the hydrophobic part of the polymer. This result also explains, on one hand, the very small dimensional changes which accompany the swelling process, and on the other hand, the fact that the absence of modification of the SANS spectra upon swelling can be considered as a confirmation that the swelling only consists of the filling of the ionic domains.

IV. Conclusions

Several series of sulfonated polyimide polymers were synthesized and studied for structural investigation. The results emanating either from the scattering profiles or from the ^{1}H NMR spectra indicate that no structure evolution accompanies the swelling process. The SANS and SAXS profiles are identical, thus suggesting that the system can be analyzed as a two-phase system: the ionic domains containing a homogeneous distribution of the polymer chain wearing the ionic groups and the polymeric matrix. Furthermore, the effect of the charge content is not very important, while the effect of the charge distribution is very pronounced. Despite the existence of large ionic domains, the SPI 6-6 membranes do not present the ionomer peak. This result is attributed to the rigidity of the polymer chain, which prevents the organization of the ionic domains. This conclusion is supported by the fact that an ionomer peak is observed when the neutral aromatic diamine is replaced by an aliphatic diamine, introducing thus some flexibility into the SPI 6-6 polymer chain. Moreover, the rigidity of the neutral sequence governs the reorganization of the structure much more than that of the ionic sequence. Finally, in the case of SPI 5-5 membranes, it was found that the local order model reproduces satisfactorily the experimental data.

Acknowledgment. We thank José Teixera, our contact at Laboratoire Léon Brillouin, and Pierre Lesieur, our contact at LURE, for their help. We are also grateful to Jacques Lambard (CEA-Saclay) for the USAXS experiments.

Note Added after ASAP Posting. This article was posted ASAP on 12/31/2003. Changes have been made to refs 23 and 25. The correct version was posted on 01/15/2004.

References and Notes

(1) Pineri, M.; Eisenberg, A. *Structure and properties of ionomers*; D. Reidel Publishing Co.: Dordrecht, Holland, 1987.
(2) Schlick, S. *Ionomers: characterization, theory and applications*; CRC Press: Boca Raton, FL, 1996.
(3) Eisenberg, A. *Macromolecules* **1970**, *3*, 147.
(4) Dreyfus, B. *Macromolecules* **1985**, *18*, 284.
(5) Longworth, R.; Vaughan, D. *Polym. Prepr. (Am. Chem. Soc., Div. Polym. Chem.)* **1968**, *9*, 525.
(6) Boyle, N. G.; McBrierty, V. J.; Douglass, D. C. *Macromolecules* **1983**, *16*, 75.
(7) Pilar, J.; Labsky, J.; Schlick, S. *Phys. Chem* **1995**, *99*, 12947.
(8) Szajdzinska-Pietek, E.; Pilar, J.; Schlick, S. *J. Phys. Chem.* **1995**, *99*, 313.
(9) Rankothge, M.; Moran, H. G.; Hook, J.; Van Gorkom, L. *Solid State Ionics* **1994**, *67*, 241.
(10) Macknight, W. J.; Taggart, W. P.; Stein, R. S. *J. Polym. Sci., Polym. Symp.* **1974**, *45*, 113.
(11) Gierke, T. D.; Munn, G. E.; Wilson, F. C. *J. Polym. Sci., Polym. Phys. Ed.* **1981**, *19*, 1687.
(12) Williams, C. E.; Russel, T. P.; Jérôme, R.; Horrion, J. *Macromolecules* **1986**, *19*, 2877.
(13) Gouin, J. P.; Bossé, F.; Nguyen, D.; Williams, C. E.; Eisenberg, A. *Macromolecules* **1993**, *26*, 7250−7255.
(14) Faure, S. Ph.D. Thesis, Joseph Fourier University-Grenoble 1, 1996.
(15) Vallejo, E.; Pourcelly, G.; Gavach, C.; Mercier, R.; Pineri, M. *J. Membr. Sci.* **1999**, *160*, 127.

(16) Zhang, Y.; Litt, M.; Savinell, R. F.; Wainrigth, J. S. *Polym. Prepr. (Am. Chem. Soc., Div. Polym. Chem.)* **1999**, *40* (2), 480.
(17) Cornet, N.; Diat, O.; Gebel, G.; Jousse, F.; Marsacq, D.; Mercier, R.; Pineri, M. *J. New Mater. Electrochem. Syst.* **2000**, *3*, 33.
(18) Genies, C.; Mercier, R.; Sillion, B.; Cornet, N.; Gebel, G.; Pineri, M. *Polymer* **2001**, *42*, 359.
(19) Guo, X.; Fang, J.; Watari, T.; Tanaka, K.; Kita, H.; Okamoto, K. *Macromolecules* **2002**, *35*, 6707.
(20) Blachot, J. F.; Diat, O.; Putaux, J. L.; Rollet, A. L.; Rubatat, L.; Vallois, C.; Müller, M.; Gebel, G. *J. Membr. Sci.* **2003**, *214*, 31.
(21) Faure, S.; Mercier, R.; Aldebert, P.; Pinéri, M.; Sillon, B. French Patent 96 05707, 1996.
(22) Faure, S.; Cornet, N.; Gebel, G.; Mercier, R.; Pinéri, M.; Sillon, B. In *Proceedings of the 2nd International Symposium on New Materials for Fuel Cell and Modern Battery Systems*; Savadogo, O., Roberge, P. R., Eds.; Montreal, Canada, 1997; p 818.
(23) Alexander, L. E.; Eisman, G. A. U.S. Patent 4 802 960, 1986.
(24) Wycisk, R.; Pintauro, P. Sulfonated polyphosphazene ion-exchange membranes *J. Membr. Sci.* **1996**, *119*, 155.
(25) Steck, A.; Stone, C. In *Proceedings of the 2nd International Symposium on New Materials for Fuel Cells and Modern Battery Systems*; Savadogo, O., Roberge, P. R., Eds.; Montreal, Canada, 1997; p 792.
(26) Zaidi, S. M. J.; Mikhailenko, S. D.; Robertson, G. P.; Guiver, M. D.; Kaliaguine, S. *J. Membr. Sci.* **2000**, *173*, 17.
(27) Pourcelly, G.; Oikonomou, A.; Gavach, C. *J. Electroanal. Chem.* **1990**, *287*, 43−59.
(28) Lambard, J.; Zemb, T. *J. Appl. Crystallogr.* **1991**, *24*, 555.
(29) Lambard, J.; Lesieur, P.; Zemb, T. *J. Phys. I* **1992**, *2*, 1191.
(30) Dreyfus, B.; Gebel, G.; Aldebert, P.; Pineri, M.; Escoubes, M.; Thomas, M. *J. Phys. (Paris)* **1990**, *51*, 1341.
(31) Porod, G.; Glatter, O.; Kratky, O. *Small-Angle X-ray Scattering*; Academic Press: London, 1982.
(32) Gebel, G.; Lambard, J. *Macromolecules* **1997**, *30*, 7914−7920.
(33) Rollet, A. L.; Diat, O.; Gebel, G. *J. Phys. Chem. B* **2002**, *106*, 12.
(34) Ding, Y. S.; Hubbard, S. R.; Hodgson, K. O.; Register, R. A.; Cooper, S. L. *Macromolecules* **1988**, *21*, 1698.
(35) Chu, B.; Wang, J.; Li, Y.; Peiffer, D. G. *Macromolecules* **1992**, *25*, 4229.
(36) Dreyfus, B.; Pinéri, M.; Eisenberg, A. *Structure and properties of ionomers*; D. Reidel Publishing Co.: Dordrecht, Holland, 1987.
(37) Gebel, G.; Moore, R. B. *Macromolecules* **2000**, *33*, 4850−4855.
(38) Dreyfus, B. In *Structure and properties of ionomers*; Pineri, M., Eisenberg, A., Eds.; NATO ASI Series C-198; D. Reidel Publishing Co.: Dordrecht, Holland, 1987; pp 27−37.
(39) Volino, F.; Pinéri, M.; Dianoux, A. J.; de Geyer, A. *J. Polym. Sci., Polym. Phys. Ed.* **1982**, *20*, 481.
(40) Schlick, S.; Gebel, G.; Pineri, M.; Volino, F. *Macromolecules* **1991**, *24*, 3517.
(41) Avalos, J.; Gebel, G.; Pineri, M.; Volino, F.; Schlick, S. *Polym. Prepr. (Am. Chem. Soc., Div. Polym. Chem.)* **1993**, *34*, 448.
(42) Schlick, S.; Gebel, G. In *Ionomers: characterization, theory and applications*; Schlick, S., Ed.; CRC Press: Boca Raton, FL, 1996; p 165.

MA034965P